

## Double-Well States of *Ungerade* Symmetry in H<sub>2</sub>: First Observation and Comparison with *Ab Initio* Calculations

A. de Lange, W. Hogervorst, and W. Ubachs

*Laser Center, Department of Physics and Astronomy, Vrije Universiteit,  
De Boelelaan 1081, 1081 HV Amsterdam, The Netherlands*

L. Wolniewicz

*Nicholas Copernicus University, 87-100 Torun, Poland*

(Received 23 October 2000)

The observation of a new class of long-lived outer well states of *ungerade* symmetry ( $B''\bar{B}^1\Sigma_u^+$ ) in molecular hydrogen, lying above the ionization threshold, is reported. Rovibrational levels within a potential extended over internuclear separations of  $R = 7\text{--}25$  a.u. are experimentally investigated in a triple resonance scheme. Good agreement ( $<0.5\text{ cm}^{-1}$ ) with updated *ab initio* calculations is found for vibrational levels up to  $v = 26$ , demonstrating that such calculations can now be extended to this energetic range above ionization, as long as interaction with the Rydberg manifolds is shielded by a barrier. The dynamical behavior (predissociation and autoionization) of this class of “*u*” symmetry states is remarkably different from similar outer well states of “*g*” symmetry; this phenomenon can be understood from the structure of doubly excited electronic states.

DOI: 10.1103/PhysRevLett.86.2988

PACS numbers: 33.80.Eh, 31.15.Ar, 33.20.Ni, 33.80.Rv

H<sub>2</sub>, consisting of two protons and two electrons, is the simplest neutral molecule. However, because the nuclei in H<sub>2</sub> are so light, the usual approximations made in the calculation of potential energy curves and level energies (Born-Oppenheimer and adiabatic approximations) have a strong tendency to be invalid, thus complicating *ab initio* calculations. Additional effects of the low mass are the large spacings between vibrational and rotational levels, to an extent that the optical spectrum of H<sub>2</sub> has no obviously discernible regularities. It is for these reasons that the majority of emission lines of H<sub>2</sub>, as observed in discharge spectra and tabulated in the *Dieke atlas* [1], is still unassigned.

As a result of the strong couplings between singly excited states ( $1s\sigma_g$ ) ( $n\ell\lambda_{u,g}$ ), forming Rydberg progressions below the first ionization threshold, the doubly excited states (with both electrons in  $n \geq 2$ ) and the  $H^+ + H^-$  ion-pair configuration, the potential energy curves of the singlet states may adopt a double-well structure. For the electronic states of singlet character and *g*-inversion symmetry this is the rule rather than the exception. Levels in the lowest  $EF^1\Sigma_g^+$  state were first observed by Dieke [2,3], whereas the double-well structure of this state was first recognized by Davidson [4]. Kołos and Wolniewicz [5] performed an accurate *ab initio* calculation and the dynamical properties (tunneling) in the double-well structure were studied by Senn and Dressler [6]. Later laser excitation of the  $EF^1\Sigma_g^+$  state was studied by Kligler *et al.* [7] and Marinero *et al.* [8]. While the third adiabatic state of  $^1\Sigma_g^+$  symmetry ( $GK^1\Sigma_g^+$ ) has a less pronounced barrier, a series of levels entirely confined in the outer well of the fourth  $^1\Sigma_g^+$  state ( $H\bar{H}^1\Sigma_g^+$ ) was observed by our group via multistep laser excitation [9]. This paper deals with the first observation of a double-well state of *u* symmetry.

Notwithstanding the specific problems, the hydrogen molecule is used as the pivotal test system for detailed comparison between spectroscopic observation and *ab initio* calculation of molecular properties. Generally most theoretical approaches use explicit two-electron correlated wave functions [10]. The methods of calculating potential energy curves and level energies break down at highly elevated energies, because of the large number of electronic configurations involved. For this reason *ab initio* calculations cannot be extended to the energy region approaching the ionization limit. As an alternative the method of multi-channel-quantum-defect theory (MQDT) has been developed, specifically for H<sub>2</sub> in a first principles fashion, approaching the problem of the excited states downwards from the ionization limit. Encouraging results have been obtained [11,12], but it should be noted that these results also depend on *ab initio* calculations of the potential curves of the lower electronic states. It is the purpose of this joint experimental/theoretical study to explore the validity of accurate adiabatic *ab initio* calculations in the energetic range of the ionization threshold.

The existence of the  $B''\bar{B}^1\Sigma_u^+$  double-well state in H<sub>2</sub> was predicted by Dabrowski and Herzberg [13], while a calculation of its Born-Oppenheimer potential was reported by Kołos [14]. Here we report an updated calculation along with the first observation and calibration of singly resolved rovibrational levels using laser excitation. Since the levels of the outer well (referred to as  $\bar{B}^1\Sigma_u^+$ ) are confined to large internuclear separation ( $R \geq 7$  a.u.), there is no Franck-Condon overlap with the  $X^1\Sigma_g^+$ ,  $v = 0$  ground state, which prohibits direct excitation. A method of consecutive excitation using three tunable lasers allows for overlap in steps, exploiting large wave function density

at classical inner and outer turning points of the potentials, as shown in Fig. 1. Three electric dipole transitions are then required to reach levels of  $u$  symmetry from the ground state.

Important aspects of the experimental setup have been described in previous publications [9,15]. Wavelength-tunable extreme ultraviolet (XUV) radiation was produced by third-harmonic generation in a xenon jet using the frequency-doubled output of a pulsed dye laser. Throughout this study the XUV output was fixed at the  $B^1\Sigma_u^+ - X^1\Sigma_g^+$  (15,0)  $R(1)$  transition, populating the  $B^1\Sigma_u^+$  ( $v = 15, J = 2$ ) rovibrational state. A second pulsed laser (tunable in the near infrared at 870 nm) further excited the  $H_2$  molecules into the  $I'^1\Pi_g, v = 0, J = 1-3$  states, by probing either one of the  $P(2), Q(2)$  and  $R(2)$  transitions. This two-photon excited intermediate  $I'^1\Pi_g$  state has the advantage that it is long-lived ( $\tau > 100$  ns) and that its wave function density at small internuclear distances is negligible. The latter property ensured that in a third laser excitation step only states at large internuclear distances were probed.

The third laser, for which another Nd:YAG pumped pulsed dye laser, tunable in the range  $\lambda = 780-970$  nm was used, exploited the population of the  $I'^1\Pi_g$  state to probe the rovibrational levels in the  $\bar{B}^1\Sigma_u^+$  state. Finally, a fourth laser at 532 nm was used to reach the dissociation continuum of the molecular ion, generating  $H^+$  ions for signal detection (see Fig. 1). These ions were accel-

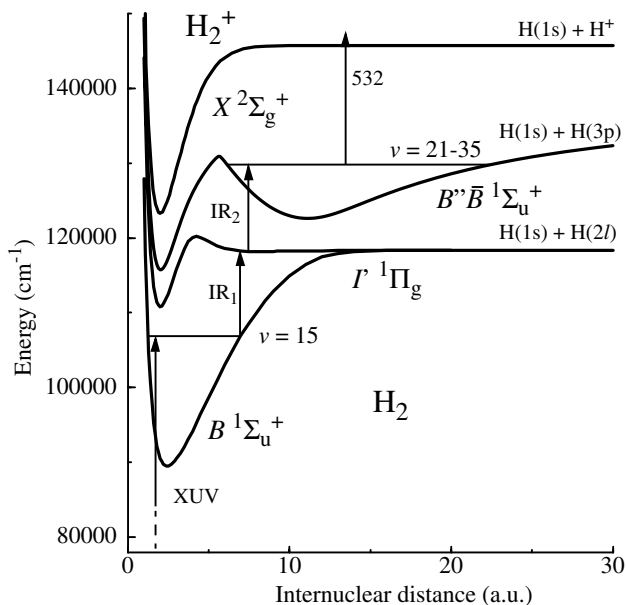


FIG. 1. The four-laser excitation scheme employed to probe the  $\bar{B}$  outer well state in molecular hydrogen in the sequence  $X^1\Sigma_g^+ - B^1\Sigma_u^+ - I'^1\Pi_g - \bar{B}^1\Sigma_u^+$  with a fourth laser for the production of  $H^+$  ions after reaching the dissociation continuum of  $H_2^+$ . The final two laser pulses are delayed in time by  $\approx 50$  ns with respect to the first two, to discriminate the signal from background ions produced in the first two steps.

erated and collected at an electron multiplier mounted in a time-of-flight drift tube for mass selection. A typical recording, using the  $I'^1\Pi_g, v = 0, J = 3(e)$  state as intermediate, and probing the  $\bar{B}, v = 29$  level is shown in Fig. 2.

To extract level energies in the  $\bar{B}$  state with respect to the  $X^1\Sigma_g^+$  ( $v = 0, J = 0$ ) ground state, only the third laser has to be calibrated, because the levels in the shallow outer well of the  $I'^1\Pi_g$  state were already calibrated to within several  $0.01 \text{ cm}^{-1}$  [15]. In the near infrared no calibration standard is available and therefore part of the laser radiation is frequency doubled to record a  $Te_2$  spectrum [16] yielding absolute accuracies of  $\approx 0.05 \text{ cm}^{-1}$ . In regions where no  $Te_2$  reference is available the accuracy is only  $\approx 0.2 \text{ cm}^{-1}$ .

An accurate potential energy curve for the  $B''\bar{B}$  state including adiabatic corrections was reported earlier [17]. Here we computed the relativistic corrections to this curve using the same method as applied to the  $H\bar{H}$  state [18], i.e., the relativistic corrections were determined from the covalent part of the electronic wave function (the corrections are available via the internet [19]). In the range of relevant internuclear separations  $R = 5-25$  a.u. this relativistic correction varies between  $1.1$  and  $1.5 \text{ cm}^{-1}$ . This corrected potential was used in the vibrational Schrödinger equation to extract vibration-rotational energies,  $E_{v,J}$  with respect to the  $2H^+ + 2e^-$  limit. From these the theoretical term values,  $T_{v,J}$  with respect to the  $v = 0, J = 0$  ground state of  $H_2$ , were determined as

$$T_{v,J} = E_{v,J} - 2E_H + D_0(H_2) + \Delta E_{\text{rad}}, \quad (1)$$

where  $E_H = -109\,678.7717 \text{ cm}^{-1}$  is the theoretical H atom ground state energy [20] and  $D_0(H_2) = 36\,118.069 \text{ cm}^{-1}$  the  $H_2$  ground state dissociation energy [21]. The last term in Eq. (1) is the radiative correction to  $E_{v,J}$ . We assume this to be equal to the radiative correction for the  $H^-$  ion, i.e.,  $\Delta E_{\text{rad}} = 0.274 \text{ cm}^{-1}$  [22]. This is certainly a reasonable assumption for the vibrational levels in the outer minimum of the potential curve.

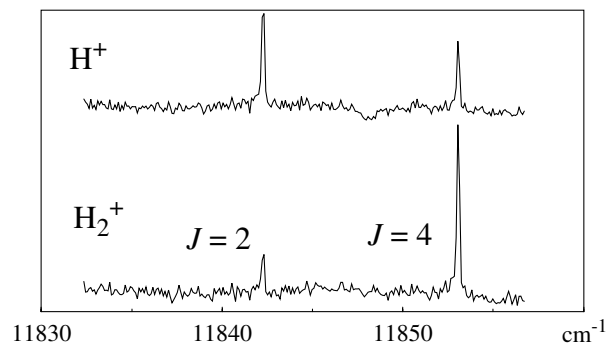


FIG. 2. Excitation spectrum of the  $\bar{B}, v = 29$  level in molecular hydrogen, using the  $I'^1\Pi_g, v = 0, J = 3(e)$  as an intermediate. Simultaneous  $H^+$  (generic signal) and  $H_2^+$  (signal from autoionization) recordings are shown in the upper and lower trace vs the frequency of the laser used in the third step.

The three-step excitation scheme was used to probe and calibrate vibrational levels  $\nu = 21\text{--}35$  in the  $\bar{B}$  outer well. Results are listed in Table I, along with deviations from *ab initio* values. With the XUV laser fixed to the  $R(1)$  transition, for reasons of signal strength, only *ortho*-levels in  $\bar{B}^1\Sigma_u^+$  were probed ( $J = 0, 2, 4$ ). The numbering of vibrational quantum levels pertains to the subset associated with the outer well. The series of levels  $\nu = 21\text{--}26$ , all lying  $4000\text{ cm}^{-1}$  above the ionization threshold, are well described (within  $0.5\text{ cm}^{-1}$ ) by the *ab initio* calculation. It is expected that also the vibrational levels  $\nu = 0\text{--}20$ , not accessible in the present setup, follow the theoretical description, since for this part of the potential no perturbations will occur. Up to vibrational levels  $\nu = 30$  a gradually increasing downward shift with respect to calculation is found, but the assignments remain

TABLE I. Observed and calculated level energies. Accuracies  $\approx 0.05\text{ cm}^{-1}$  for  $\nu = 23\text{--}29$  and  $\approx 0.2\text{ cm}^{-1}$  for  $\nu = 21, 22$ , and  $30\text{--}35$ .

| $J$        | $T_{\text{obs}}$ | $\Delta_{\text{o-c}}$ | $J$        | $T_{\text{obs}}$ | $\Delta_{\text{o-c}}$ |
|------------|------------------|-----------------------|------------|------------------|-----------------------|
| $\nu = 21$ |                  |                       | $\nu = 22$ |                  |                       |
| 0          | 128 597.01       | +0.20                 | 0          | 128 803.41       | +0.48                 |
| 2          | 128 602.36       | +0.46                 | 2          | 128 808.61       | +0.65                 |
| 4          | 128 614.34       | +0.59                 | 4          | 128 820.30       | +0.63                 |
| $\nu = 23$ |                  |                       | $\nu = 24$ |                  |                       |
| 0          | 129 004.28       | +0.29                 | 0          | 129 200.23       | +0.08                 |
| 2          | 129 009.23       | +0.26                 | 2          | 129 205.15       | +0.09                 |
| 4          | 129 020.78       | +0.23                 | 4          | 129 216.63       | +0.13                 |
| $\nu = 25$ |                  |                       | $\nu = 26$ |                  |                       |
| 0          | 129 391.37       | -0.13                 | 0          | 129 577.84       | -0.56                 |
| 2          | 129 396.24       | -0.15                 | 2          | 129 582.62       | -0.59                 |
| 4          | 129 407.54       | -0.16                 | 4          | 129 593.77       | -0.51                 |
| $\nu = 27$ |                  |                       | $\nu = 28$ |                  |                       |
| 0          | 129 759.65       | -1.08                 | 0          | 129 937.10       | -1.63                 |
| 2          | 129 764.41       | -1.05                 | 2          | 129 941.75       | -1.64                 |
| 4          | 129 775.52       | -1.01                 | 4          | 129 952.70       | -1.55                 |
| $\nu = 29$ |                  |                       | $\nu = 30$ |                  |                       |
| 0          | 130 110.12       | -2.39                 | 0          | 130 278.56       | -3.38                 |
| 2          | 130 114.75       | -2.39                 | 2          | 130 283.61       | -3.11                 |
| 4          | 130 125.55       | -2.31                 | 4          | 130 294.60       | -2.83                 |
| $\nu = 31$ |                  |                       | $\nu = 32$ |                  |                       |
| 0          | 130 444.89       | -7.09                 | 0          | 130 604.75       | -7.19                 |
| 2          | 130 449.29       | -0.66                 | 2          | 130 609.36       | -7.62                 |
| 4          | 130 458.95       | -3.87                 | 4          | 130 620.08       | -2.31                 |
| $\nu = 33$ |                  |                       | $\nu = 34$ |                  |                       |
| 0          | 130 761.51       | -8.82                 | 0          | 130 914.10       | -11.00                |
| 2          | 130 766.02       | -8.90                 | 2          | 130 918.73       | -10.93                |
| 4          | 130 776.72       | -10.17                | 4          | 130 929.26       | -11.13                |
| $\nu = 35$ |                  |                       |            |                  |                       |
| 0          | 131 061.79       | -13.93                |            |                  |                       |
| 2          | 131 066.91       | -13.62                |            |                  |                       |
| 4a         | 131 072.64       | -18.59                |            |                  |                       |
| 4b         | 131 084.34       | -6.89                 |            |                  |                       |

unambiguous and no local perturbations occur; such effects would result in  $J$ -dependent shifts. A gradual shift can originate from slight inaccuracies in the potential and from increasing nonadiabatic interactions.

At  $\nu = 31$  up to  $\nu = 35$  erratic behavior sets in, which is related to the increase of wave function densities at short internuclear distances, where interactions with Rydberg and doubly excited states occur. In Fig. 3 expectation values  $\langle R \rangle$  as calculated from the obtained wave functions are plotted (for  $J = 0$ ). The deviation at  $\nu = 31$  marks the coupling behavior, which obscures the assignment of states to either one of the wells. At higher  $J$  the  $\nu = 31$  levels cross with those of  $\nu = 9$  from the inner well and strong mixing occurs, giving rise to level shifts. For higher vibrational levels ( $\nu > 35$ ), still some assignments can be made although a vibrational quantum number associated with the outer well loses its meaning. Around the expected value for the level energy of  $\nu = 35, J = 4$ , two lines are observed (both listed in Table I) as a result of a near coincidence between levels with wave function density in either well.

For the vibrational levels  $\nu \geq 29$ ,  $\text{H}_2^+$  ions are generated simultaneously with  $\text{H}^+$ . This indicates that autoionization competes with excitation by the 532 nm laser pulse. For the higher vibrational levels ( $\nu > 32$ ), autoionization resulting in  $\text{H}_2^+$  is the only observable process. The experimental setup is not sensitive for predissociation into the  $\text{H}(n=2) + \text{H}$  channel. The  $B''\bar{B}$  state couples nonadiabatically to Rydberg states and ionization continua at small  $R$  and the picture of the adiabatic potentials break down. However, the coupling distorts mainly the wave functions

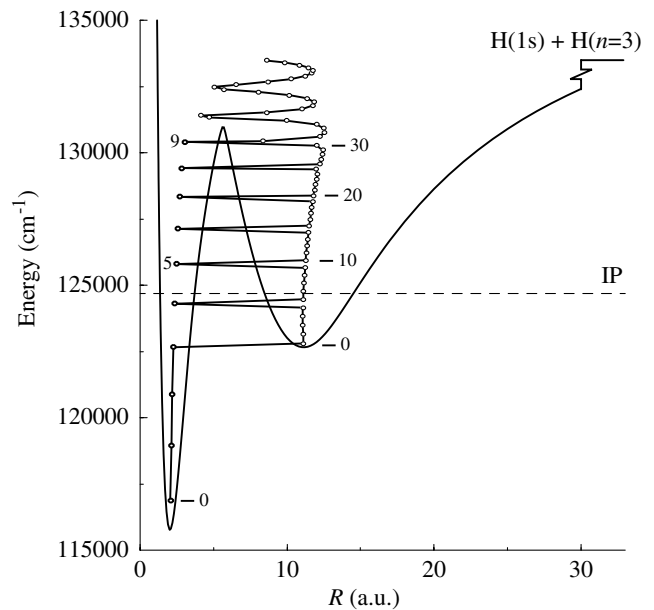


FIG. 3. Potential curve of the  $B^1\Sigma_u^+$  state and the expectation values  $\langle R \rangle$  calculated for  $J = 0$  wave functions. Vibrational numbering is given separately for the inner and outer well states. At  $\nu = 31$  a severe deviation is found due to large wave function density at small internuclear distances.

at small internuclear distances, leaving the wave functions at larger distances virtually unaffected, and vibrational levels assigned to the outer well can still be described within this framework. The lifetime of such a state is governed by the probability to find a molecule at small internuclear distances where it can autoionize. Generally, close to the top of the potential barrier, the wave function density of levels associated with the outer well will also obtain sizable values in the inner well. This results in shorter lifetimes and line broadening effects are expected. However, up to the highest  $\nu$  no broadening beyond  $0.1 \text{ cm}^{-1}$  (laser linewidth) is observed.

This behavior for the  $u$  symmetry  $B''\bar{B}^1\Sigma_u^+$  state is markedly different from the  $g$  symmetry state of nearly equal shape ( $H\bar{H}^1\Sigma_g^+$ ); in the latter case linewidths up to  $1.5 \text{ cm}^{-1}$  are observed [9]. This difference in dynamical behavior of the outer well states of  $u$  and  $g$  symmetry is related to the global potential structure of  $u$  and  $g$  singlet states. For the *gerade* singlet states the first doubly excited state  $(2p\sigma)^2$  comes down to the energetic range below the  $n = 2$  limit [23]. This repulsive state, which in the adiabatic picture is associated with the  $F^1\Sigma_g^+$  outer well state, largely governs the fast decay in the  $g$  manifold giving rise to strong predissociation into  $H(n = 2)$  products. For the  $u$ -singlet states the lowest doubly excited state converges to  $n = 3$  and its asymptote falls energetically above the range studied here. Hence the decay for  $u$  states is primarily governed by vibrational and rotational autoionization into the Rydberg manifolds of  $u$  symmetry, whereas predissociation plays a minor role. This explains the lower decay rates.

In conclusion the observed levels in the lowest outer well of  $u$  symmetry are represented perfectly (within  $0.5 \text{ cm}^{-1}$ ) by adiabatic *ab initio* calculations, even at excitation energies  $4000 \text{ cm}^{-1}$  above the ionization threshold. Only in the upper  $1000 \text{ cm}^{-1}$  below the barrier some deviations are found that may be related to a slight misrepresentation of the potential near the barrier. At the point where strong coupling with states at small  $R$  sets in the adiabatic representation naturally breaks down; here nonadiabatic shifts due to interaction with Rydberg manifolds prevail; these infinite numbers of states are beyond the scope of present day *ab initio* calculations.

Financial support from the Netherlands Foundation for Fundamental Research of Matter (FOM) is gratefully acknowledged. The authors also thank E. Reinhold for fruitful discussions.

- 
- [1] H. M. Crosswhite, *The Hydrogen Molecule Wavelength Tables of Gerhard Heinrich Dieke* (Wiley-Interscience, New York, 1972).
  - [2] G. H. Dieke, Phys. Rev. **50**, 797 (1936).
  - [3] G. H. Dieke, Phys. Rev. **76**, 50 (1949).
  - [4] E. R. Davidson, J. Chem. Phys. **33**, 1577 (1960).
  - [5] W. Kołos and L. Wolniewicz, J. Chem. Phys. **50**, 3228 (1969).
  - [6] P. Senn and K. Dressler, J. Chem. Phys. **87**, 1205 (1987).
  - [7] D. J. Kligler and C. K. Rhodes, Phys. Rev. Lett. **40**, 309 (1978).
  - [8] E. E. Marinero, C. T. Rettner, and R. N. Zare, Phys. Rev. Lett. **48**, 1323 (1982).
  - [9] E. Reinhold, W. Hogervorst, and W. Ubachs, Phys. Rev. Lett. **78**, 2543 (1997).
  - [10] W. Kołos, Adv. Quantum Chem. **5**, 99 (1970); D. M. Bishop and L. M. Cheung, Adv. Quantum Chem. **12**, 1 (1980); J. Rychlewski, Adv. Quantum Chem. **31**, 173 (1999).
  - [11] S. C. Ross and Ch. Jungen, Phys. Rev. Lett. **59**, 1297 (1987).
  - [12] Ch. Jungen, S. T. Pratt, and S. C. Ross, J. Phys. Chem. **99**, 1700 (1995).
  - [13] I. Dabrowski and G. Herzberg, Can. J. Phys. **52**, 1110 (1974).
  - [14] W. Kołos, J. Mol. Spectrosc. **62**, 429 (1976).
  - [15] E. Reinhold, A. de Lange, W. Hogervorst, and W. Ubachs, J. Chem. Phys. **109**, 9772 (1998).
  - [16] J. Cariou and P. Luc, *Atlas du Spectre d'Absorption de la Molécule de Tellure* (Laboratoire Aime-Cotton, Orsay, 1980).
  - [17] E. Reinhold, W. Hogervorst, W. Ubachs, and L. Wolniewicz, Phys. Rev. A **60**, 1258 (1999).
  - [18] L. Wolniewicz, J. Chem. Phys. **109**, 2254 (1998).
  - [19] <http://www.phys.uni.torun.pl/ftp/publications/ifiz/luwo/re1.BB>
  - [20] G. W. Erickson, J. Phys. Chem. Ref. Data **6**, 831 (1977).
  - [21] L. Wolniewicz, J. Chem. Phys. **103**, 1792 (1995).
  - [22] C. L. Pekeris, Phys. Rev. **112**, 1649 (1958).
  - [23] S. L. Guberman, J. Chem. Phys. **78**, 1404 (1983).